

Low velocity limits of cold atom clocks

J. Muñoz,^{*} I. Lizuain,[†] and J. G. Muga[‡]

Departamento de Química-Física, UPV-EHU, Apartado Postal 644, 48080 Bilbao, Spain

Fundamental low-energy limits to the accuracy of quantum clock and stopwatch models in which the clock hand motion is activated by the presence of a particle in a region of space have been studied in the past, but their relevance for actual atomic clocks had not been assessed. In this work we address the effect of slow atomic quantum motion on Rabi and Ramsey resonance fringe patterns, as a perturbation of the results based on classical atomic motion. We find the dependence of the fractional error of the corresponding atomic clocks on the atomic velocity and interaction parameters.

PACS numbers: 03.65.Xp, 03.65.Ta, 06.30.Ft

I. INTRODUCTION

There is a sizable amount of work devoted to “quantum clocks” in which a clock “hand” variable runs during the passage of a particle through a region of space [1, 2, 3, 4, 5, 6, 7, 8, 9, 10, 11, 12, 13], see an extensive review in [14]. Much of this work is related to the “Larmor clock” for an electron crossing a potential barrier and the determination of tunneling times [15], but even the timing of a simple freely-moving particle poses intriguing questions [16]. In principle, and from a classical-mechanical perspective, reading the hand after the particle has crossed the region (the particle may also be put at time $t = 0$ *within* the region) should provide a measurement of the time that the particle has spent there. The method faces though a low energy limit to its accuracy because the interaction between the particle and the clock perturbs the particle and thus the measurement. This limitation was formulated by Peres [3, 5] as a bound of the time resolution of the clock τ (the time required to distinguish two orthogonal hand states),

$$\tau E > \hbar, \quad (1)$$

for a given particle energy E . The same result follows by imposing that the transmission probability be close to 1 [10]; it has been also found without reference to any clock from Kijowski’s time-of-arrival distribution [17], τ being in this case the time-of-arrival uncertainty and E the average incident energy; and quite interestingly, it arises as well as a decoherence condition for consistent histories in the analysis of Halliwell and Yearsley of the quantum time of arrival [18]. If, encouraged by the agreement of so many different approaches, we apply this inequality to the energy of a Cesium atom moving at speeds of conventional Cs clock standards (between 100 and 300 m/s), the predicted resolution is $\sim 10^{-14}$ s, which is consistent with accuracies achieved in the 70’s and 80’s but it is

an order of magnitude too large for more recent conventional Cs clocks [19]. If, instead, we assume a velocity of 5 cm/s, one of the smallest speeds projected so far for a Cs atom clock in space [20], the resulting minimal “resolution” is a worryingly high $0.36 \mu\text{s}$, many orders of magnitude larger than the stated target accuracy of 10^{-16} s for that clock. In fact current cold-atom fountain clocks provide accuracies much better than the ones that follow from Eq. (1). Clearly the naive application of Eq. (1) is not justified, but the question remains as to what the negative effect is, if any, of very low atomic motion on atomic clocks.

Quite independently of the works on “quantum clocks”, time-frequency metrology has experienced a phenomenal progress. Precisely, one of the main factors for recent and future accuracy improvement is laser cooling and the concomitant use of low atomic velocities [19] to make flight times large and the resonance curve narrower. Therefore there is indeed a need to evaluate fundamental low energy limits for atomic clocks [21, 22]. The characteristic quantum clock process described above (the particle activating a handle in a space region), is similar to the physical basis of an atomic clock but there are some important differences as well: in a simple atomic clock with a one-field (Rabi) configuration, an atom in the ground state passes through a field region in resonance with a hyperfine atomic transition, which induces the internal excitation of the atom. Since the ground or excited state populations oscillate periodically with Rabi’s frequency Ω when an atom at rest is immersed in the field, it is natural, except possibly for too low energies, to relate the passage time to the final internal oscillation phase, which can be read out from the excited population. In the atomic clock, however, the quantity of interest is not really the passage time, even though it plays an important role, but the frequency of the transition. This is determined from the central peak of the resonance curve, whose width is inversely proportional to the passage time as we shall see in more detail: an analysis where the transition of the atom across the field is treated classically, which is valid when the atomic kinetic energy $E = k^2\hbar/(2m)$ is larger than other relevant energy scales, $E \gg \hbar\Delta, \hbar\Omega/2$, (Δ is the detuning, m the

^{*}Electronic address: josemunoz@saitec.es

[†]Electronic address: dirk.seidel@ehu.es

[‡]Electronic address: jg.muga@ehu.es

mass, and $\hbar k/m$ the velocity), shows that the probability of excitation to level 2, when the incident atom is in the ground state 1 and the field width is l , is given by

$$P_{12}^{scl}(\Delta) = \frac{\Omega^2}{\Omega^2 + \Delta^2} \sin^2 \left(\frac{\sqrt{\Omega^2 + \Delta^2} T}{2} \right), \quad (2)$$

where $T = lm/(\hbar k)$ is the (classical) in-field flight-time. Three relevant properties of P_{12} are the mentioned narrowing of the main peak when T increases, the peak at $\Delta = 0$ irrespective of the atomic velocity (or equivalently of T), and the symmetry around $\Delta = 0$. Thus, velocity averaging does not affect the central fringe much, so that measurement of P_{12} can be used to steer the frequency of an external oscillator close to the reference, ideally unperturbed atomic frequency ω_0 . This steering will be more accurate the narrower the peak, i.e., for slower atoms. The clockwork then produces the second by counting a predetermined number of oscillations of the external oscillator, $\approx 9.2 \times 10^9$ for Cs clocks, so that a shift in the peak translates into an error in the determination of the second of the order of the fractional frequency error.¹

Most atomic clocks actually use the Ramsey configuration with two separated fields rather than one, to improve performance, but the above three properties of P_{12} remain true also for the Ramsey scheme. In the Ramsey scheme the free-flight time between fields plays the role of T as the parameter to be maximized, within technical constraints, for narrowing the resonance. We shall first restrict the study to the Rabi configuration for simplicity, and provide later the results for the Ramsey configuration, since the manipulations are very similar but lengthier. Our main aim is to determine the fractional frequency error of the clock at “low” incident velocities: this is the (absolute value of the) shift of the peak of $P_{12}(\Delta)$ with respect to the ideal value $\Delta = 0$ divided by the atomic transition frequency. The term “low velocity” here is subtle and must be clarified: we shall consider velocities where the semiclassical result (with the peak at $\Delta = 0$) has to be *corrected* perturbatively because of quantum motion, but such that the overall interference pattern keeps essentially the same form as for the semiclassical limit. Physically this means that reflection from the field regions is still very unlikely and $E \gg \Omega \hbar$. This will enable us to find the corrections by solving first the quantum dynamics exactly and then, taking the dominant and first correction terms in “large k ” expansions. An example of the perturbative regime is provided in Fig. 1a, where the quantum curve resembles, but it is slightly perturbed with respect to, the semiclassical curve. We insist that this regime may in fact involve very small velocities according to other criteria, such as the velocities in Fig. 1a, unrealistically low in any actual atomic

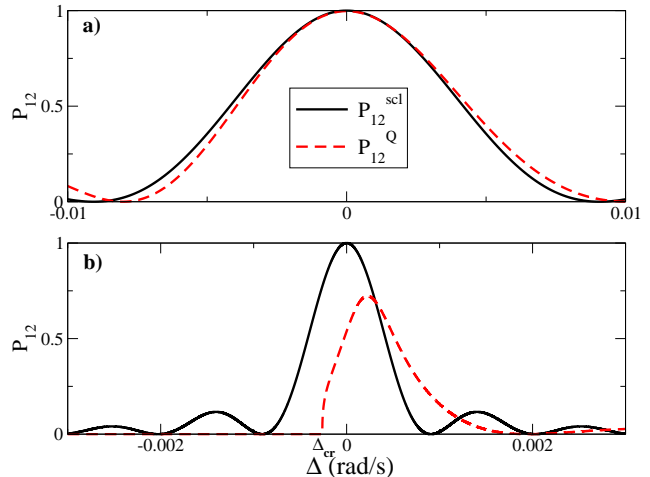


FIG. 1: (Color online) Rabi (one-field) scheme. (a) Perturbative regime: the maximum probability of the exact and semiclassical solutions P_{12}^Q and P_{12}^{scl} practically coincide at $\Delta = 0$ for a π -pulse. Note however the peak asymmetry and the related shift at half height. Data: $l = 3$ mm and $v = 5$ $\mu\text{m/s}$. (b) Reflection-dominated regime: the central fringe is narrower and severely deformed ($v = 0.5$ $\mu\text{m/s}$, note the different scale), and starts from a critical detuning. In (a) and (b) The Rabi frequency is fixed by the π -pulse condition $\Omega = \pi v/l$. The mass of Cs is used in all figures: $m(\text{Cs}) = 2.2 \times 10^{-25}$ Kg.

clock, but useful for illustrating clearly the main features of the quantum curve, in particular the asymmetry, and the maximum very near $\Delta = 0$, at least for the naked eye (the maximum is in fact shifted but only slightly as discussed in more detail later on).

Reflection from the field becomes relevant for $E \leq \Omega/\hbar$, but then the interference pattern is drastically deformed. For a Ramsey configuration this implies a multiple scattering scenario with entirely new Fabry-Perot resonances highly sensitive to the velocity [21] and the existence of a threshold of P_{12} with respect to detuning. This very extreme regime, see an example in Fig. 1b, is out the scope of current time-frequency metrology so we shall instead concentrate on the perturbative regime.

The objective is to evaluate $P_{12}(\Delta)$ quantally for the transmitted atoms. We shall use as a simplified model the effective 1D Hamiltonian

$$\hat{H} = \frac{\hat{p}^2}{2m} - \hbar \Delta |2\rangle\langle 2| + \frac{\hbar}{2} \Omega(x) (|1\rangle\langle 2| + |2\rangle\langle 1|), \quad (3)$$

which is obtained, see [23, 24], by assuming a semiclassical effective traveling wave field, and applying rotating wave and dipolar approximations. The effective microwave field may be realized by two copropagating lasers perpendicular to the atomic motion which induce a Raman transition [25, 26]. In this case the effective de-

¹ unless of course it is well understood and predictable so that it can be corrected by hand.

tuning Δ contains, apart from the difference between effective laser frequency (difference between the copropagating laser frequencies) and transition frequency, the recoil term $-k_L^2 \hbar / (2m)$, k_L being the effective wavenumber (difference between the two laser wavenumbers). Finally, $\Omega(x)$ is the effective Rabi frequency that we consider to be constant in the illuminated region(s) and zero outside.

To find the exact solution of Eq. (3) we start by solving the stationary Schrödinger equation (SSE) for each zone labeled with an index α : on the left of the field ($\alpha = I$), in the field ($\alpha = II$), and on the right of the field ($\alpha = III$):

$$\hat{H}_\alpha \phi_\alpha = E \phi_\alpha; (\alpha = I, II, III), \quad (4)$$

where ϕ_α is a two-component wavevector

$$\phi_\alpha = \begin{pmatrix} \phi_\alpha^{(1)} \\ \phi_\alpha^{(2)} \end{pmatrix}. \quad (5)$$

i) For $\alpha = I$,

$$\left(\frac{\hat{p}^2}{2m} - \hbar \Delta |2\rangle\langle 2| \right) \phi_I = E \phi_I \quad (6)$$

reduces to two uncoupled equations for $\phi_I^{(1)}$ and $\phi_I^{(2)}$. The general solution (delta-normalized in k space) is thus

$$\begin{aligned} \phi_I = & \frac{1}{\sqrt{2\pi}} [(a_I e^{ikx} + b_I e^{-ikx})|1\rangle \\ & + (c_I e^{iqx} + d_I e^{-iqx})|2\rangle], \end{aligned} \quad (7)$$

where $q = \sqrt{k^2 + 2m\Delta/\hbar}$ and $k = \sqrt{2mE/\hbar^2}$.

ii) For the interaction region, $\alpha = II$,

$$\left[\frac{\hat{p}^2}{2m} - \hbar \Delta |2\rangle\langle 2| + \frac{\hbar}{2} \Omega (|1\rangle\langle 2| + |2\rangle\langle 1|) \right] \phi_{II} = E \phi_{II}. \quad (8)$$

By diagonalizing the interaction part of the Hamiltonian we obtain its wave vectors and eigenstates $|\lambda_\pm\rangle$,

$$|\lambda_\pm\rangle = \begin{pmatrix} 1 \\ \frac{2\lambda_\pm}{\Omega} \end{pmatrix}, \quad (9)$$

where $\lambda_\pm = \frac{-\Delta \pm \Omega'}{2}$ and $\Omega' = \sqrt{\Delta^2 + \Omega^2}$.

From Eq. (11) and (9) we may write the solution of the SSE in $\alpha = II$ as

$$\begin{aligned} \phi_{II} = & \frac{1}{\sqrt{2\pi}} [(a_{II} e^{ik_+x} + b_{II} e^{-ik_+x})|\lambda_+\rangle \\ & + (c_{II} e^{ik_-x} + d_{II} e^{-ik_-x})|\lambda_-\rangle], \end{aligned} \quad (10)$$

with the mode wavenumbers obeying

$$\frac{\hbar^2 k_\pm^2}{2m} = \frac{\hbar^2 k^2}{2m} - \hbar \lambda_\pm. \quad (11)$$

iii) Finally, for $\alpha = III$ we have, as for $\alpha = I$,

$$\begin{aligned} \phi_{III} = & \frac{1}{\sqrt{2\pi}} [(a_{III} e^{ikx} + b_{III} e^{-ikx})|1\rangle \\ & + (c_{III} e^{iqx} + d_{III} e^{-iqx})|2\rangle]. \end{aligned} \quad (12)$$

In all cases, $\alpha = I, II, III$, it is useful to introduce the vector of coefficients

$$\mathbf{v}_\alpha = (a_\alpha, b_\alpha, c_\alpha, d_\alpha)^\mathcal{T}, \quad (13)$$

where \mathcal{T} means “transpose”.

II. TRANSFER MATRICES AND EXCITATION PROBABILITY

Let us consider a plane wave $\frac{1}{\sqrt{2\pi}} e^{ikx}$, incident from the left ($x \rightarrow -\infty$), with the atoms in the ground state $|1\rangle$ so that $a_I = 1$, $c_I = 0$, $b_{III} = d_{III} = 0$. After the interaction “barrier”, the transmitted atom traveling to $x \rightarrow \infty$ may stay in $|1\rangle$ or be excited in $|2\rangle$, so that

$$\begin{aligned} \mathbf{v}_I &= (1, r_{11}, 0, r_{12})^\mathcal{T}, \\ \mathbf{v}_{III} &= (t_{11}, 0, t_{12}, 0)^\mathcal{T}, \end{aligned} \quad (14)$$

where r_{ij}, t_{ij} are reflection and transmission amplitudes for left incidence in internal state $i = 1, 2$ and outgoing internal state $j = 1, 2$.

Let us now introduce for the outer regions, $\alpha = I, III$, a vector containing the amplitudes and their derivatives,

$$\begin{pmatrix} \phi_\alpha^{(1)}(x) \\ \phi_\alpha^{(2)}(x) \\ \dot{\phi}_\alpha^{(1)}(x) \\ \dot{\phi}_\alpha^{(2)}(x) \end{pmatrix} = M_0(x) \mathbf{v}_\alpha, \quad (15)$$

and similarly, inside the field ($\alpha = II$)

$$\begin{pmatrix} \phi_{II}^{(1)}(x) \\ \phi_{II}^{(2)}(x) \\ \dot{\phi}_{II}^{(1)}(x) \\ \dot{\phi}_{II}^{(2)}(x) \end{pmatrix} = M_b(x, \phi_1) \mathbf{v}_{II}, \quad (16)$$

where the dot represents derivative with respect to x . The explicit form of the matrices $M_0(x)$ and $M_b(x)$ is

$$M_0(x) = \frac{1}{\sqrt{2\pi}} \begin{pmatrix} e^{ikx} & e^{-ikx} & 0 & 0 \\ 0 & 0 & e^{iqx} & e^{-iqx} \\ ike^{ikx} & -ike^{-ikx} & 0 & 0 \\ 0 & 0 & iqe^{iqx} & -iqe^{-iqx} \end{pmatrix} \quad (17)$$

$$M_b(x) = \frac{1}{\sqrt{2\pi}} \begin{pmatrix} \frac{e^{ik_+x}}{2\lambda_+e^{ik_+x}} & \frac{e^{-ik_+x}}{2\lambda_+e^{-ik_+x}} & \frac{e^{ik_-x}}{2\lambda_-e^{ik_-x}} & \frac{e^{-ik_-x}}{2\lambda_-e^{-ik_-x}} \\ \frac{\Omega}{ik_+e^{ik_+x}} & \frac{\Omega}{-ik_+e^{-ik_+x}} & \frac{\Omega}{ik_-e^{ik_-x}} & \frac{\Omega}{-ik_-e^{-ik_-x}} \\ \frac{2ik_+\lambda_+e^{ik_+x}}{\Omega} & \frac{-2ik_+\lambda_+e^{-ik_+x}}{\Omega} & \frac{2ik_-\lambda_-e^{ik_-x}}{\Omega} & \frac{-2ik_-\lambda_-e^{-ik_-x}}{\Omega} \end{pmatrix} \quad (18)$$

The matching conditions at x_1 and x_2 for the wave functions and their derivatives can now be written as

$$M_0(x_1)\mathbf{v}_I = M_b(x_1)\mathbf{v}_{II}, \quad (19)$$

$$M_b(x_2)\mathbf{v}_{II} = M_0(x_2)\mathbf{v}_{III}. \quad (20)$$

Eliminating \mathbf{v}_{II} from the system above, we end up with a transfer matrix $\mathbf{T}(x_1, x_2, \phi_1)$ which connects the amplitude vectors of both sides,

$$\mathbf{v}_I = \mathbf{T}(x_1, x_2)\mathbf{v}_{III}, \quad (21)$$

and is given by the matrix product

$$\mathbf{T}(x_1, x_2) = M_0(x_1)^{-1}M_b(x_1)M_b(x_2)^{-1}M_0(x_2). \quad (22)$$

Using Eqs. (14,17,18) we may calculate the transmission amplitude for passing from $|1\rangle$ to $|2\rangle$ from the left as

$$t_{12} = \frac{\mathbf{T}_{31}}{\mathbf{T}_{31}\mathbf{T}_{13} - \mathbf{T}_{33}\mathbf{T}_{11}}. \quad (23)$$

The exact quantum excitation probability is thus, generalizing the semiclassical result (2),

$$P_{12}^Q(\Delta) = \frac{q}{k} |t_{12}|^2. \quad (24)$$

III. QUANTUM MOTION SHIFTS

Two different shifts will be considered, $\Delta_Q^{(M)}$ and $\Delta_Q^{(hh)}$: the first one is the shift of the maximum of the resonance peak with respect to $\Delta = 0$; the second one is the shift of the average between the resonance curve points at half height. As hinted by Fig. 1a they have quite a different behavior, the first one being negligible for the naked eye whereas the second one is clearly significant. We shall provide analytical expressions for the former, and numerical results for the later.

We shall first calculate the maximum value of $P_{12}^Q(\Delta)$. From

$$\frac{dP_{12}^Q}{d\Delta} = 0 \quad (25)$$

and Eq. (24), the maximum must satisfy

$$t_{12}t_{12}^* + \frac{q^2\hbar}{m} \left(\frac{dt_{12}}{d\Delta}t_{12}^* + t_{12}\frac{dt_{12}^*}{d\Delta} \right) = 0. \quad (26)$$

The explicit expression in terms of the basic variables v, L, Ω is long and cumbersome, since each element \mathbf{T}_{ij} of the matrix $\mathbf{T}(x_1, x_2)$ in Eq. (23) results from multiplying four matrices 4×4 . To simplify we shall first eliminate Ω by imposing $\Omega = \frac{\hbar k \pi}{Lm}$, which is the semiclassical condition for a π -pulse at $\Delta = 0$, and then expand t_{12} in powers of Δ up to second order,

$$t_{12,\Delta} \approx \gamma_0(k) + \gamma_1(k)\Delta + \gamma_2(k)\Delta^2, \quad (27)$$

where

$$\gamma_0 = [t_{12}]_{\Delta=0} \quad (28)$$

$$\gamma_1 = \left[\frac{\partial t_{12}}{\partial \Delta} \right]_{\Delta=0} \quad (29)$$

$$\gamma_2 = \frac{1}{2} \left[\frac{\partial^2 t_{12}}{\partial \Delta^2} \right]_{\Delta=0}. \quad (30)$$

The probability $P_{12}^Q(\Delta)$ is approximately

$$P_{12}^Q(\Delta) = \frac{q}{k} |(\gamma_0 + \gamma_1\Delta + \gamma_2\Delta^2)|^2. \quad (31)$$

Substituting the expansions in Eq. (26),

$$\begin{aligned} & |(\gamma_0 + \gamma_1\Delta + \gamma_2\Delta^2)|^2 + \\ & 2q^2 \frac{\hbar}{m} \text{Re}[(\gamma_1 + 2\gamma_2\Delta)(\gamma_0 + \gamma_1\Delta + \gamma_2\Delta^2)^*] = 0. \end{aligned} \quad (32)$$

Gathering terms, truncating in first order of Δ and using

$$\begin{aligned} \theta_0(k) &= \gamma_0\gamma_0^* + q^2 \frac{\hbar}{m} (\gamma_1\gamma_0^* + \gamma_0\gamma_1^*) \\ \theta_1(k) &= (\gamma_1\gamma_0^* + \gamma_0\gamma_1^*) + 2q^2 \frac{\hbar}{m} (\gamma_1\gamma_1^* + \gamma_2\gamma_0^* + \gamma_0\gamma_2^*) \end{aligned}$$

the peak must satisfy

$$\theta_0(k) + \theta_1(k)\Delta + \mathcal{O}(\Delta^2) = 0,$$

which can be solved retaining the dominant order in k to find the explicit shift expression

$$\Delta_Q^{(M)}(k) = \frac{\hbar^2 \pi^4}{16m^2 v l^3} \sin(2kl), \quad (33)$$

where $v = \hbar k/m$ is the velocity, see Fig. 2a, and the superscript M stands for “maximum”.

We may proceed similarly for the Ramsey configuration and write down a new transfer matrix which is of course more complicated but in principle explicit with

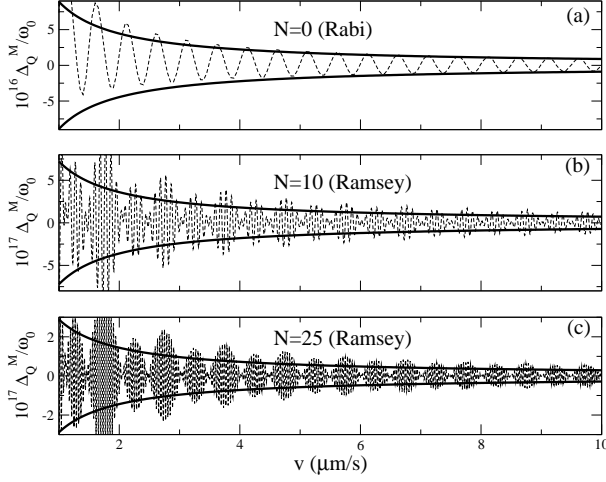


FIG. 2: Comparison between numerical (dashed lines) and analytical values (solid lines), of Δ_Q over the transition frequency ω_0 for a Cs atom at different velocities. (a) Single Rabi π -pulse with $l = 3$ mm, Rabi frequency fixed by π -pulse condition, $\Omega = \pi v/l$. For the analytical results only upper/lower bounds of Eq. (33) have been plotted. The approximations are better for higher velocities. (b) and (c) Ramsey $\pi/2$ pulses with $l = 1.5$ mm and separated by L , ($N = L/l$), Rabi frequency fixed by $\pi/2$ -pulse condition, $\Omega = \pi v/2l$.

the aid of a program of algebraic manipulation. This new transfer matrix depends on the previous parameters and on L , the length between fields. For “large” k , a large ratio $N = L/l$, and imposing $\pi/2$ pulses at each field, now $\Omega = \frac{\hbar k \pi}{2lm}$, we find the approximate envelope

$$(\Delta_Q^{(M)})_{env} = \pm \frac{\hbar^2 \pi^2}{16m^2 v l^3 N}. \quad (34)$$

Note that the Ramsey shifts are considerably smaller than Rabi shifts because of the N in the denominator. Compared to the Rabi case, the shift for the Ramsey configuration oscillates with respect to k with a short period π/L , superimposed to the long period π/l , see Fig. 2b,c. These shifts are in any case rather small and, in addition, they oscillate rapidly with respect to v so that they will average out because of the velocity spread of the atomic cloud.

There is however a second type of shift which is quite relevant in practice: it is defined as the average of the resonance curve detunings at half height of the central peak, $\Delta_Q^{(hh)}$. We numerically find out that the resonance peak is asymmetric and that, at variance with the former definition, this shift does not oscillate around zero but it tends to a constant at “large” k for fixed l and L .

As shown e.g. in Fig. 1a, this shift is more significant than the former, both because of its larger magnitude and because of the absence of oscillation with respect to velocity, see Fig. 3. Note that the quantum excitation curve

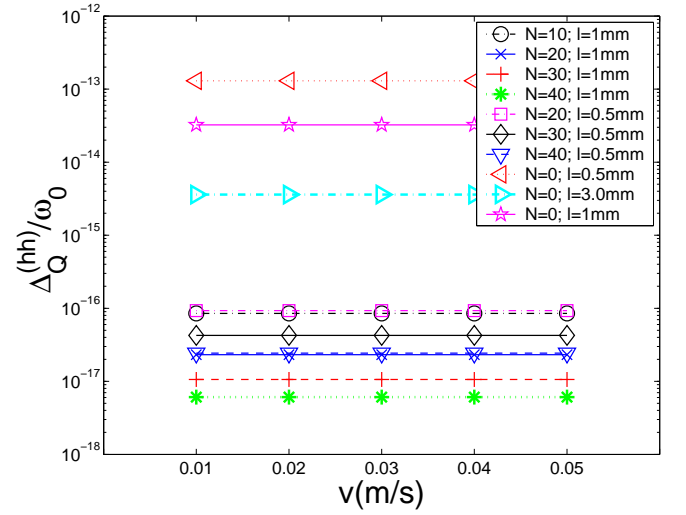


FIG. 3: (Color online) Constant values of the fractional frequency offset for the Rabi ($N = 0$) and Ramsey configurations versus incident velocity for different values of l and $N = L/l$. Exact results.

tends to the semiclassical curve when compared “vertically” for increasing v and for a given Δ , $P_{12}^Q - P_{12}^{scl} \rightarrow 0$. This is compatible with the fact that, when compared “horizontally” at half height, the two curves are separated by a shift which stays constant when increasing v . If we represent only the central peak, this constant shift is less and less visible due to the peak broadening and changing scale when v increases. A back-of-the-envelope argument may help to gain some intuitive understanding of this phenomenon giving relevant dependences. First notice that the wavenumber q is not an even function with respect to Δ and provides asymmetry: the excited atom finds a lower potential ground with positive detuning than with negative detuning and the quantum excitation probability at half height may be approximated as $(q/k)P^{scl}$, see Eq. (24), or simply $q/(2k)$, larger than $1/2$ for positive detuning and smaller otherwise. Expanding for large k , and approximating Δ as half the distance to the first zero, the vertical difference between quantum and semiclassical curves at half height is, for the Rabi scheme, $\approx \pi/(4kl)$. On the other hand the slope, again estimated from the zero and for the Rabi case is $\approx lm/(\hbar k \pi)$. As this slope is also the ratio between vertical and horizontal shifts, there results a k -independent horizontal shift proportional to l^{-2} for Rabi excitation², or to L^{-2} for Ramsey excitation and large N . This dependences are confirmed in Figs. 3, 4, and 5.

² The full predicted shift is $\hbar \pi^2 / (4ml^2)$ which provides remarkably good results given the roughness of the argument.

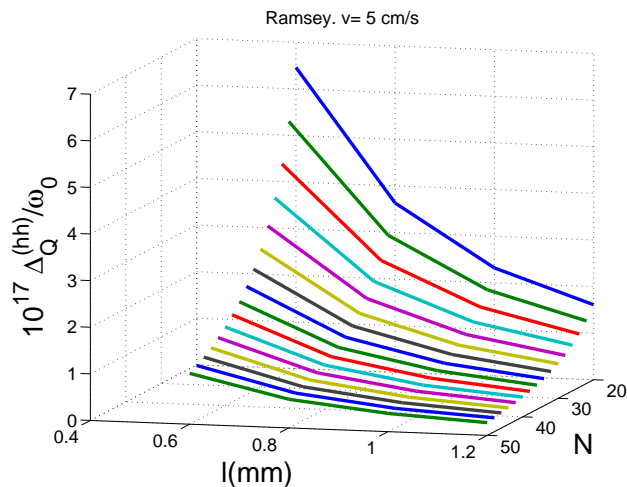


FIG. 4: (Color online) Fractional frequency offset versus l and $N = L/l$ for $v = 5$ cm/s. Exact results

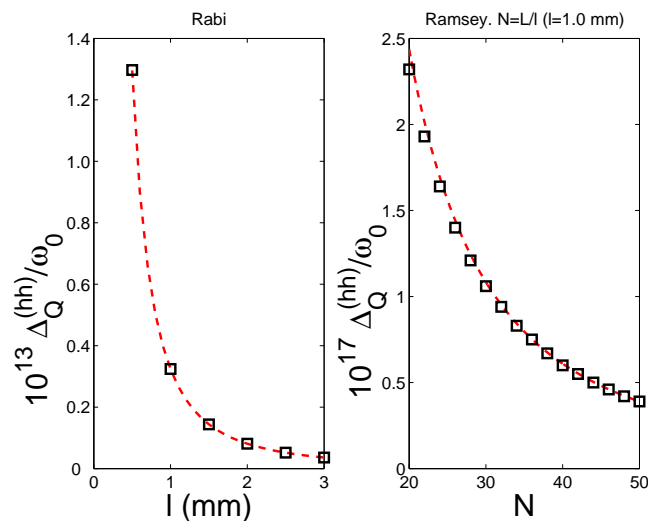


FIG. 5: (Color online) Fractional frequency offset at half height versus l and $N = L/l$ for $v = 5$ cm/s. Exact results (squares) and fits to an inverse square form (dashed).

IV. CONCLUSIONS

The bound for the time resolution of a quantum clock, Eq. (1), suggests limitations to the accuracy of atomic clocks at low atomic velocities. One of the derivations of

Eq. (1) relies on the reflection of particles from the interacting field. For an atomic beam crossing a field near resonance this means $E \gg \Omega \hbar$, which is reminiscent of Peres' bound. However $1/\Omega$ does not play at all the role of the time resolution of an atomic clock, which is nowadays even much better than the oscillation period of the atomic transition, a modest 10^{-10} Hz. Motivated by the facts that a naive application of Eq. (1) does not provide a valid assessment of actual low energy limits of atomic clocks, and that nevertheless, the trend to use lower and lower atomic velocities requires this type of information, we have investigated resonance shifts in atomic clock configurations of Rabi and Ramsey type due to quantum atomic motion. Explicit expressions are provided for the shift of the maximum, Eqs. (33) and (34), but this effect is quite small compared to the peak asymmetry, and moreover it would cancel out because of averaging over incident velocities. Instead, when the resonance is defined by the middle point of the resonance peak at half height, the peak asymmetry implies a significant shift, several orders of magnitude larger than the shift of the maximum, and robust with respect to momentum averaging. Both shifts are smaller in the Ramsey scheme than in the Rabi scheme, but even so the half-height asymmetry shift would have to be considered in the error budget of accurate Raman-Ramsey clocks. It can be reduced by increasing the width of the interaction region between field and atom, and, in the Ramsey scheme, by increasing the free-flight length. The present results motivate further work to investigate similar effects in standing wave rather than traveling wave configurations and for smooth field intensities.

Finally, we would like to comment on atomic clock designs based on trapped ions and illumination pulses in time rather than fixed in space. As the ion is trapped, it might seem that such a scheme is free from quantum-motion shifts but this is not the case. We have provided expressions for the corresponding shifts in [27].

Acknowledgments

We are very grateful to R. Wynands for useful comments on the manuscript. This work has been supported by Ministerio de Educación y Ciencia (FIS2006-10268-C03-01) and the Basque Country University (UPV-EHU, GIU07/40).

-
- [1] A. Baz', Sov. J. Nucl. Phys. **4**, 182 (1967).
 - [2] V. Rybachenko, Sov. J. Nucl. Phys. **5**, 635 (1967).
 - [3] A. Peres, Am. J. Phys. **48**, 552 (1980).
 - [4] M. Büttiker, Phys. Rev. A **27**, 6178 (1983).
 - [5] A. Peres, Quantum Theory: Concepts and Methods, Kluwer Academic, New York, (1995), Chap. 12.
 - [6] C. R. Leavens, Solid State Commun. **86**, 781 (1993).
 - [7] C. R. Leavens and W. R. McKinnon, Phys. Lett. **194**, 12 (1994).
 - [8] C. Bracher, J. Phys. B: At. Mol. Opt. Phys. **30**, 2717 (1997).
 - [9] C. R. Leavens and R. Sala Mayato, Ann. Phys. Leipzig **7**, 662 (1998).
 - [10] Y. Aharonov, J. Oppenheim, S. Popescu, B. Reznik, and

- W.G. Unruh, Phys. Rev. A **57**, 4130 (1998).
- [11] A. Casher, B. Reznik, Phys. Rev. A **62**, 042104 (2000).
 - [12] D. Alonso, R. Sala Mayato, and J. G. Muga, Phys. Rev. A **67**, 032105 (2003).
 - [13] D. Sokolovski, Phys. Rev. A **76**, 042125 (2007).
 - [14] R. Sala Mayato, D. Alonso, and I.L. Egusquiza, Lect. Notes Phys. **734**, 235 (2008).
 - [15] M. Büttiker, Lect. Notes Phys. **734**, 279 (2008).
 - [16] J. Muñoz, D. Seidel, and J. G. Muga, Phys. Rev. A **79**, 012108 (2009).
 - [17] A. D. Baute, R. Sala Mayato, J. P. Palao, J. G. Muga, and I. Egusquiza, Phys. Rev. A **61**, 022118 (2000).
 - [18] J. J. Halliwell and J. M. Yearsley, arXiv:0903.1957.
 - [19] J. Vanier and C. Audoin, Metrologia **42**, S31 (2005).
 - [20] Ph. Laurent et al., Eur. Phys. J. D **3**, 201 (1998); Ch. Salomon et al., C.R. Acad. Sci. Paris Serie IV **2**, 1313(2001).
 - [21] D. Seidel and J. G. Muga, Eur. Phys. J. D **41**, 71 (2007).
 - [22] S. V. Mousavi, A. del Campo, I. Lizuain, and J. G. Muga, Phys. Rev. A **76**, 033607 (2007).
 - [23] I. Lizuain, S. V. Mousavi, D. Seidel, J. G. Muga, Phys. Rev. A **78**, 013633 (2008).
 - [24] A. Ruschhaupt and J. G. Muga, Phys. Rev. A **76**, 013619, (2007).
 - [25] J. E. Thomas et al., Phys. Rev. Lett. **48**, 867 (1982).
 - [26] J. Vanier, Appl. Phys. B **81**, 421 (2005).
 - [27] I. Lizuain, J. G. Muga and J. Eschner, Phys. Rev. A **76**, 033808 (2007).